Geophysical Journal International

Geophys. J. Int. (2020) **223,** 1338–1354
Advance Access publication 2020 August 10
GJI Seismology

doi: 10.1093/gji/ggaa368

The signal of outermost-core stratification in body-wave and normal-mode data

Rûna van Tent,[1,2] Arwen Deuss,[1] Satoshi Kaneshima[3] and Christine Thomas[2]

[1]*Department of Earth Sciences, Utrecht University, Heidelberglaan* 8, 3584 *CS Utrecht, The Netherlands. E-mail: r.m.vantent@uu.nl*
[2]*Institute of Geophysics, University of Münster, Münster, Germany*
[3]*Department of Earth and Planetary Sciences, Kyushu University, Fukuoka* 819-0395, *Japan*

Accepted 2020 July 29. Received 2020 July 15; in original form 2020 January 16

SUMMARY

Seismological models of the outer core's radial velocity structure show that the outermost core is slower than PREM. For models derived from body-wave data these low velocities are confined to the top of the outer core, while normal-mode data prefer a velocity gradient that deviates from PREM throughout the entire outer core. These different models have led to conflicting interpretations regarding the presence of stratification at the top of the outer core. While body-wave based models have been shown to require a compositionally stratified outermost core, the velocity and density profiles obtained from normal-mode data correspond to a homogeneous outer core. In addition, the observed low velocities in the outermost core are difficult to reconcile with compositional models of stratification, as the required enrichment in light elements would generally increase seismic velocities. Here, we investigate how well-suited both seismic body-wave and normal-mode data are to constrain the velocity and density structure of the outer core. To this end, we model and compare the effects of outer-core structure and D″ structure on the differential traveltimes of body-wave phases SmKS and on the centre frequencies of normal modes. We find that a trade-off between outer-core structure and D″ structure exists for both data types, but neither data can be readily explained by reasonable D″ velocities and densities. Low outermost-core velocities are therefore still required by seismological data. Using additional information from the centre frequencies of Stoneley modes—normal modes that are particularly sensitive to variations in velocity and density at the top of the outer core—we confirm that normal-mode data indeed require low velocities with respect to PREM in the outermost core, similar to a recent normal-mode model, and an overall higher outer-core density. The presence of buoyant stratification in the outermost core is therefore not immediately supported by the centre frequencies of Stoneley modes. Stratification with high seismic velocity, as one would expect from most straightforward stratification-forming processes, is directly contradicted by our results.

Key words: Composition and structure of the core; Body waves; Surface waves and free oscillations.

1 INTRODUCTION

Earth's liquid outer core is considered approximately homogeneous in composition, as a result of the vigorous convection that is required to sustain the geodynamo that generates Earth's magnetic field. In a well-mixed outer core, elastic properties change with increasing pressure along an adiabatic gradient as defined by an equation of state (EoS). Assuming adiabatic conditions, deviations of the velocity and density gradients from the self-compression profiles defined by the EoS may be used as indicators of compositional heterogeneity (Birch 1952) in the outermost core (e.g. Kaneshima & Helffrich 2013).

Seismological studies have reported anomalously low seismic velocities in the outermost core since the 1970s (Hales & Roberts 1971) and 1990s (Lay & Young 1990; Souriau & Poupinet 1991; Garnero *et al.* 1993; Tanaka & Hamaguchi 1993) and have argued that these low velocities may be attributed to the presence of compositionally distinct material, implying the presence of buoyant stratification in the outermost core. But not only seismic data indicate a stratified outer core: other observations that appear to require outermost-core stratification are fluctuations in the Earth's magnetic field with a period of approximately 60 yr that can best be explained by weaker, thermal stratification, as opposed to stronger, compositional stratification (Buffett *et al.* 2016). Thermal

stratification of the outermost core has been proposed by Mound *et al.* (2019) as the result of reduced heat extraction from the core under hot mantle regions, that is, the large low shear velocity provinces (LLSVPs, e.g. Lay 2015) in the lower mantle underneath Africa and the Pacific. Regional subadiabatic conditions would then allow for the formation of thermal stratification, resulting in a laterally heterogeneous outermost core. The presence of laterally heterogeneous thermal stratification in the outermost core is supported by Olson *et al.* (2018), who compared numerical geodynamo models for a stratified outer core to existing models of the magnetic field at the core–mantle boundary. Davies *et al.* (2015) also predict a thermally stratified outermost core, based on core-evolution models that use high, experimentally determined electrical and thermal conductivities of Fe–Si–O mixtures at core conditions.

All hypotheses on the formation of buoyant, compositional stratification involve the presence of light elements, as a lower density in the outermost core is required to stabilize any liquid stratification against convection. Chemical interactions across the core–mantle boundary may for example enrich the outermost core in light elements (Knittle & Jeanloz 1991), although compositional stratification may even form without an external source of light elements. Barodiffusion, the process where light elements are transported from higher to lower pressures by means of diffusion, may have been responsible for the accumulation of light elements at the top of the outer core immediately following the differentiation of the core (Gubbins & Davies 2013). Recently, Arveson *et al.* (2019) experimentally determined the pressure-temperature range where Fe–Si–O and Fe–Si would be immiscible in the outer core by extrapolating the results from laser-heated diamond-anvil cell experiments to outer-core conditions with molecular dynamics simulations. They show that the outer-core geotherm may lie within the immiscible domain, so that differentiation of Fe–Si–O and Fe–Si results in the formation of an oxygen-rich top layer.

A wide range of hypotheses has been proposed regarding the formation of outermost-core stratification, an overview of which is given in Table 1. However, it has proven difficult to reconcile predictions for the velocity and density of thermal and compositional outermost-core stratification with the actual seismic observations. For compositional stratification the difficulty lies in the enrichment of the outermost core in light elements, which reduces the density of the mostly iron core. The compressibility is affected to a lesser degree, resulting in an increase in seismic velocity (e.g. fig. 1 of Badro *et al.* 2014) as opposed to the seismically observed low velocity in the outermost core. For example, Buffett & Seagle (2010) modelled the evolution of a stratified layer enriched in oxygen that develops through chemical diffusion across the core–mantle boundary. They predict the seismic properties of the resulting layer as showing high-velocity and low-density stratification. Arveson *et al.* (2019) find that an immiscible Fe–Si–O top layer will likely also be seismically fast, as Si partitions more into the top layer and thereby increases velocities. In fact, Brodholt & Badro (2017) show, by the simulations of Fe–Ni–S–C–O–Si binary liquids, that processes that merely add extra light elements to the outermost core (including barodiffusion) will always increase the seismic velocity there.

The formation of low-velocity and low-density stratification, as would be required to match body-wave observations and simultaneously be dynamically stable, can only be accomplished under specific circumstances. Depending on the constituents involved, non-ideal mixing of light elements in the outermost core can result in both a decrease in density and in velocity (Helffrich 2012). Non-ideal mixing of the Fe–O–S system is proposed by Helffrich & Kaneshima (2010) to explain their seismically observed low velocities in the outermost core. Assuming non-ideal mixing, Helffrich (2014) find that the mixing of the early Earth's core with that of an impactor is the most plausible origin for a compositionally stratified layer that agrees with body-wave observations. However, simulations of binary liquids under core conditions show no reason to deviate from the assumption of ideal mixing (Badro *et al.* 2014). Brodholt & Badro (2017) find that, assuming ideal mixing, slow and light stratification can be generated only through the exchange of mantle elements with the outer core. They conclude that perhaps the most feasible process resulting in light and slow stratification is that of chemical interactions across the core–mantle boundary. An FeO-rich lower mantle then exchanges oxygen with silicon from the outer core, decreasing both density and velocity in the outermost core for a specific range of initial concentrations. In order to produce an observable layer in the outermost core, diffusion rates require a partially molten lowermost mantle, as would be the case for a basal magma ocean.

While the dynamic models predict higher seismic velocities and lower density, most seismic studies find low velocities (-0.4 to -0.8 per cent with respect to PREM for recent models) at the top of the outer core. The seismic body waves used to image the low velocities at the top of the outer core (SmKS waves, *S* waves that travel through the core as *P* waves and bounce $m-1$ times at the CMB, Fig. 1a), however, also travel through the heterogeneous mantle (e.g. Garnero 2000). Hence, their traveltimes and amplitudes will likely be affected by the mantle, where variations in velocity may be up to ± 2 per cent. Normal modes are also affected by mantle structure. A question therefore remains how much seismic waves are affected by mantle structure and therefore how suitable they are to provide trustworthy results of seismic properties of the outer core. Here, we will assess the ability of seismic body-wave and normal-mode data to constrain the velocity and density structure of the outer core. Since the detectability of outermost-core stratification may be particularly affected by seismic structures in the D″ region (Bullen 1950), we will quantify these effects and determine whether there is any trade-off with outer-core structure. Then, as we have determined whether seismology really does require a low-velocity outermost core, we will evaluate the stratification-forming processes listed in Table 1 based on the agreement between their expected seismic properties and the actual seismological observations.

To represent the velocity and density structure of the outer core required by seismological data, we will use two recent models: body-wave based velocity model KHOMC (Kaneshima & Helffrich 2013) and normal-mode based velocity and density model EPOC-Vinet (Irving *et al.* 2018), both shown in Figs 1(b) and (c). KHOMC is one of several recent body-wave models of the outermost core, others include those from Tanaka (2007), Alexandrakis & Eaton (2010) and Tang *et al.* (2015). KHOMC and most other models contain low velocities with respect to PREM (Dziewonski & Anderson 1981) directly below the core–mantle boundary. Alexandrakis & Eaton (2010) form the exception, as their best-fitting model is similar to PREM and requires no stratification in the outermost core. We will use KHOMC as representative of the outermost-core velocity required by body waves. This model is based on large-scale array measurements and its features have been verified with independent data sets in later publications (Kaneshima & Matsuzawa 2015) and (Kaneshima 2018), Figs S1 and S2 of the Supporting Information). KHOMC and the models from Tanaka (2007) and Tang *et al.* (2015) differ in the strength of negative v_p perturbation and depth-extent of the low velocities with respect to PREM, but

Table 1. Overview of recent outer-core studies. The top section lists studies that used seismological or magnetic field observations to study the outer core; the bottom section lists studies that predict outer-core properties by means of modelling and experiments. Outermost-core velocity and density for the seismic studies are indicated with respect to PREM, expected properties of outermost-core stratification may be with respect to any reference model that represents a well-mixed, homogeneous outer core.

Method	Outermost-core v_p	Outermost-core ρ	Stratification	Study
Outermost-core velocity profile from SmKS differential traveltimes	low	not constrained, low expected	compositional or no stratification	e.g. Garnero *et al.* (1993), Tanaka (2007), Alexandrakis & Eaton (2010), Kaneshima & Helffrich (2013), Tang *et al.* (2015)
Outer-core velocity and density profiles from normal-mode centre frequencies	low	high	no stratification	Irving *et al.* (2018)
Magnetic field observations	not constrained	low	thermal (most likely) or compositional	Buffett *et al.* (2016)
Modelling of regional stratification due to a heterogeneous CMB heat flux	not constrained	low	thermal	Mound *et al.* (2019)
Numerical geodynamo modelling compared to CMB magnetic field models	not constrained	low	thermal	Olson *et al.* (2018)
Modelling of core evolution with experimentally determined conductivities	not constrained	low	thermal	Davies *et al.* (2015)
Barodiffusion modelling	high	low	compositional	Gubbins & Davies (2013)
Fe-Si-O immiscibility from diamond-anvil cell experiments and molecular dynamics simulations	high expected	low	compositional	Arveson *et al.* (2019)
Modelling of the evolution of an oxygen-enriched layer from core–mantle interactions	high	low	compositional	Buffett & Seagle (2010)
Composition modelling to explain light and slow stratification (ideal mixing)	low	low	compositional	Brodholt & Badro (2017)
Modelling of non-ideal mixing for Fe-O-S	low	low	compositional	Helffrich (2012)
Modelling of light-element diffusion gradients to match low outermost-core velocities (non-ideal mixing)	low	low	compositional	Helffrich (2014)

they are all shown to favour a stratified outermost core. We will also compare our modelling to the data of Alexandrakis & Eaton (2010), which in their paper do not require a stratified outermost core.

EPOC-Vinet is the first outer-core model that has been obtained exclusively using normal modes (Earth's free oscillations). It contains an overall denser profile and a steeper velocity gradient compared to PREM throughout the outer core. EPOC-Vinet velocities are lower than PREM at the core–mantle boundary and slightly higher at the inner-core boundary. The velocities of EPOC-Vinet are also lower than KHOMC in the outermost core, while the gradient in velocity is slightly less steep than that of KHOMC (Fig. 1c).

Kaneshima & Helffrich (2013) find that KHOMC velocities require the presence of compositionally distinct material at the top of the outer core by showing that the steeper velocity profile deviates too strongly from the velocity gradient prescribed by the self-compression of homogeneous outer-core material according to the third-order Birch-Murnaghan equation of state. On the other hand, EPOC-Vinet's profiles were parametrized by applying the Vinet equation of state (Vinet *et al.* 1987) to the behaviour of homogeneous outer-core material, meaning that the obtained gradients inherently do not support the presence of compositional stratification. The steep velocity gradient with respect to PREM is the result of a higher compressibility of the outer-core material,

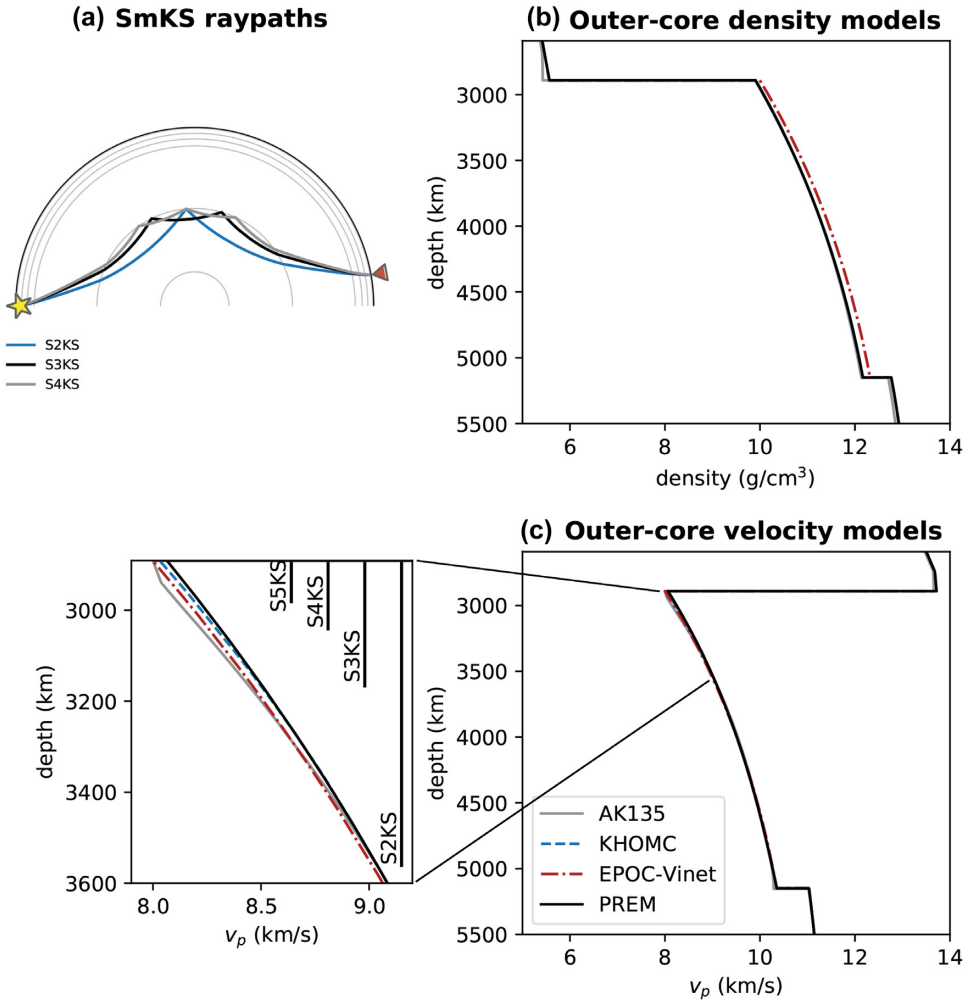

Figure 1. (a) Theoretical ray paths of SmKS waves for $m = 2, 3, 4$. The star indicates the source at 150 km depth and the triangle shows the receiver location at 170° distance. (b) and (c) respectively show several density and velocity models of the outer core (2891–5149.5 km depth): KHOMC (Kaneshima & Helffrich 2013), EPOC-Vinet (Irving *et al.* 2018), AK135 (Kennett *et al.* 1995) and PREM (Dziewonski & Anderson 1981). KHOMC is a velocity model only, PREM is used for density in the outer core. The ranges of outer-core depths sampled by the different SmKS phases are also indicated.

providing an alternative explanation for low outermost-core velocities. Thus, existing body-wave and normal-mode studies generally agree on a low-velocity outermost core but deviate as to its origin.

For our modelling, we use PREM as the reference model everywhere outside of the outer(most) core, which we replace by KHOMC and EPOC-Vinet. The outer core of PREM is approximately adiabatic (Dziewonski & Anderson 1981), although the polynomial parameterization is not based on physical properties of an outer-core composition. The (near-)adiabatic PREM profile allows for the interpretation of deviations from the PREM velocity and density profiles in the outermost core as the presence of stratification. All studies on the formation of outermost-core stratification listed in Table 1 either use PREM densities or velocities for their modelling, or show their results with respect to PREM as an example, meaning that seismic observations with respect to PREM are readily compared to the presented properties of stratification. It is important to note however, that the presence of outermost-core stratification may be considered with respect to any model that corresponds to a well-mixed, homogeneous outer-core composition.

2 METHODS

2.1 Body waves

We will use synthetic seismograms as opposed to observed data to assess the suitability of body waves to study core properties, as this allows us to control mantle structure and test its influence on traveltimes and amplitudes. The synthetic seismograms are calculated using the full-wavefield reflectivity method (Müller 1985), allowing us to identify and find the slowness of all waves that may have been affected or generated by variations in the radial structure of the outermost core and possibly find other suitable body-wave phases that may result from outermost-core stratification other than the already used SmKS. Since some of the seismic arrivals may be too small to be identified in single seismograms, the data are also examined using 4th-root vespagrams (slant stacks, Rost & Thomas 2002; Schweitzer *et al.* 2002). As we are modelling radially symmetric Earth structure, we do not have to consider topography effects or out-of-plane arrivals.

Next, we compare the effects of radial velocity structure on the differential traveltimes of SmKS waves, which are most commonly used in seismic studies to constrain outermost-core structure (e.g.

Kaneshima & Helffrich 2013). SmKS waves (Fig. 1a) are converted from S to P waves at the core–mantle boundary, travel through the outer core and reflect off the top of the outer core from below $m - 1$ times before being converted back to S waves as they re-enter the mantle. For increasing m, each phase is confined to shallower depths in the outer core.

SmKS waves are usually not studied as single phases, but by measuring the differential traveltimes $\mathrm{d}t^{m-n}$ between two phases SmKS–SnKS with respect to a reference model, for which we use PREM:

$$\mathrm{d}t^{m-n} = \left(t_m - t_n\right)_{\mathrm{data}} - \left(t_m - t_n\right)_{\mathrm{PREM}}, \tag{1}$$

where m and n indicate the phases SmKS–SnKS with traveltimes t_m and t_n.

2.2 Normal modes

The frequencies at which the entire Earth oscillates after a large earthquake ($M_{\mathrm{W}} \geq 7.5$) depend on the velocity and density structure of the Earth. Radial perturbations in v_p and ρ at the top of the outer core will slightly shift the centre frequencies of these oscillations, the Earth's normal modes. The centre frequency f_{c} of a normal mode is defined as

$$f_{\mathrm{c}} = f_0 + (4\pi)^{-\frac{1}{2}} Re\left\{ \int_0^a K_\rho(r) \left(\frac{\delta\rho(r)}{\rho(r)}\right)_0^0 + K_p(r) \left(\frac{\delta v_p(r)}{v_p(r)}\right)_0^0 + K_s(r) \left(\frac{\delta v_s(r)}{v_s(r)}\right)_0^0 \mathrm{d}r + \sum_d \delta h_0^0 H_0^d \right\}, \tag{2}$$

where f_0 is the centre frequency of the mode as calculated for the 1-D reference model (PREM). The integral on the right-hand side describes the perturbation in centre frequency as a result of a change in velocity and density structure with respect to the reference model of spherical-harmonic degree $s = 0$ and azimuthal order $t = 0$, that is radial structure. K_ρ, K_p and K_s are the mode's known sensitivity kernels to variations in ρ, v_p and v_s, respectively, and a is the radius of the Earth. The summation on the right-hand side describes the contribution of discontinuities d on the centre frequency, where δh_0^0 is the radial perturbation in the depth of the discontinuity and H_0^d is the corresponding sensitivity kernel. The centre frequency of a normal mode is by definition insensitive to 3-D structure, including discontinuity topography. We calculate centre frequencies using Mineos (Masters *et al.* 2011).

The integral in eq. (2) can be shortly written as splitting coefficient c_0^0. The c_0^0 coefficient of a normal mode is measured from normal-mode data jointly with the splitting coefficients c_s^t (e.g. Giardini *et al.* 1988) for 3-D structure of all considered degrees s. These measurements include interactions, called cross-coupling, between small groups of normal modes when they are close in frequency. Cross-coupling to modes further away in frequency is considered to be small and can be ignored in these measurements (Deuss & Woodhouse 2001). By including cross-coupling, measured c_0^0 coefficients are inherently corrected for any effect 3-D structure may have on the normal-mode data and therefore only depend on 1-D variations in the seismic model.

2.3 The frequency difference between body-wave and normal-mode data

Body-wave and normal-mode data are studied at different frequency ranges. In order to make the SmKS measurements used to create

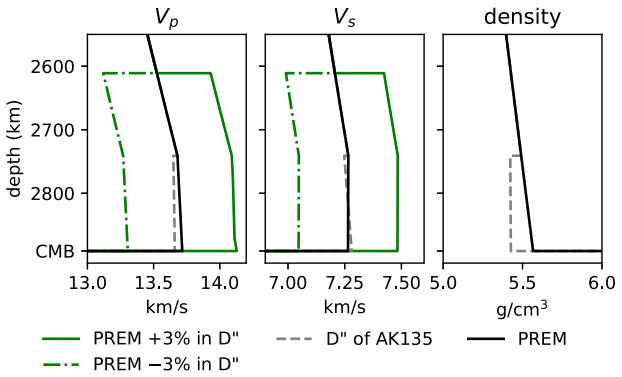

Figure 2. Models of D″ velocity and density structure used in this study. The ±3 per cent v_p and v_s models represent the range of lateral velocity variations in a 280-km-thick D″ layer. Model AK135 is used in the bottom-150 km of the mantle and represents feasible changes to PREM in average D″ velocity and density.

KHOMC, Kaneshima & Helffrich (2013) applied a bandpass filter in the range of 0.02−2 Hz to their body-wave data. The normal modes used to create the EPOC-Vinet model from Irving *et al.* (2018) have centre frequencies in the much lower range of 0.1−10 mHz. All models used in this study are valid for a reference frequency of 1 Hz, meaning that a correction of the model for dispersion due to attenuation is required for the calculation of normal-mode centre frequencies. This is done in Mineos, using

$$v_s(\mathrm{T}) = v_s(1)\left(1 - \frac{\ln \mathrm{T}}{\pi} q_\mu\right) \tag{3}$$

$$v_p(\mathrm{T}) = v_p(1)\left(1 - \frac{\ln \mathrm{T}}{\pi}[(1-E)q_\kappa + E q_\mu\right) \tag{4}$$

from Kanamori & Anderson (1977), where $v_s(1)$ and $v_p(1)$ are the shear and compressional velocity at the reference period of 1 s, T is the period to which the model is to be adjusted, $E = \frac{4}{3}(v_s/v_p)^2$ and q_κ and q_μ are the bulk and shear attenuation, respectively. Centre frequencies calculated using Mineos are therefore corrected for attenuation effects resulting from the difference between the reference frequency of the model and the frequency of the normal mode.

2.4 Modelling of outer-core and lowermost-mantle structure

Radial outer-core structure is modelled according to SmKS-based model KHOMC (Kaneshima & Helffrich 2013) and normal-mode based model EPOC-Vinet (Irving *et al.* 2018), as shown in Figs 1(b) and (c). An additional model containing a 480-km-thick outermost-core layer with a constant v_p reduction of -0.04 km s^{-1} with respect to PREM is also used. PREM is used to represent radial Earth structure outside the outer core. We quantify the effects of radial deviations from PREM in D″ on the data by changing the velocity and density profiles in D″ from PREM to AK135 (Kennett *et al.* 1995), as shown in Fig. 2.

Seismic observations have shown that the D″ region is characterized by a laterally varying discontinuity with a velocity jump of approximately 0.5–3 per cent at heights of 50–450 km above the core–mantle boundary (for reviews see: Wysession *et al.* 1998; Cobden *et al.* 2015; Lay 2015). Tomographic models such as S40RTS (Ritsema *et al.* 2011) show ±2 per cent lateral variations in v_s and slightly smaller variations in v_p near the core–mantle boundary.

Here, we use 1-D models with velocity jumps of ±3 per cent in v_p and v_s with respect to PREM at 280 km above the CMB (Fig. 2) to serve as a maximum range within which D″ velocities vary laterally in the Earth. We use these D″ models to quantify the effect of D″ velocity variations on SmKS differential traveltimes. We do not consider the effects of the ±3 per cent v_p and v_s D″ models on the centre frequencies of normal modes, as these models are a 1-D representation of 3-D heterogeneity, to which the centre frequencies are insensitive. Ultra-low velocity zones with a thickness of 40 km and with respective reductions in v_p and v_s of −10 and −30 per cent (e.g., Lay 2015) directly above the CMB are also modelled for completeness. It is beyond the scope of this study to model the full complexity of D″ structures such as topography, anisotropy and scattering heterogeneities (e.g. Garnero 2000).

3 RESULTS

First, we search for additional body-wave phases that would provide a new means to study the properties of the outermost core by checking whether any waves other than SmKS are notably affected or possibly generated by a low-velocity layer in the outermost core. Using synthetic seismograms calculated at every 0.5° between 50° and 170° for PREM and PREM with KHOMC (Kaneshima & Helffrich 2013) in the outer core, we calculate vespagrams for groups of seismograms per 10° distance. Fig. 3 contains examples of two superimposed radial-component vespagrams for the distance range of 150–160°, showing all phases that are significantly affected by KHOMC velocities. All of these phases are forms of SmKS, indicating that SmKS waves remain the most suited waves to study the velocity structure at the top of the outer core and that no new, unexpected phases are generated by imposing a lower outermost-core velocity. The depth phases of SmKS (pSmKS and sSmKS) have very similar ray paths to SmKS and show similar delays for KHOMC. The other phases (SmKSP, PSmKS and their depth phases) include an extra reflection at the surface and therefore have shorter paths in the outer core, so that their traveltimes are less affected by outer-core structure.

3.1 SmKS differential traveltimes

To analyse the effects of D″ structure on SmKS waves, we calculate synthetic seismograms and ray-theoretical arrival times for PREM with two different radial D″-models (Fig. 2): one with +3 per cent change in v_p and v_s and another with −3 per cent change in v_p and v_s in the lowermost 280 km of the mantle. Comparing the synthetic seismograms for PREM and PREM with the +3 per cent D″-layer (Fig. 4) shows that D″-structure strongly affects the arrival times and waveforms in the time interval of the SmKS arrivals, including all SmKS phases now arriving earlier. Synthetics for PREM with KHOMC in the outer core (Fig. 4) show the effect of low outermost-core velocities on the SmKS arrivals, resulting in later arrival times. While the D″ layer affects the entire trace in this time interval, the effect of low outermost-core velocities is mostly limited to the SmKS arrivals.

The data used to infer outermost-core velocity from SmKS waves are the differential traveltimes between the different *m* phases with respect to the differential times for a reference model (eq. 1), not the absolute arrival times shown in Fig. 4. Fig. 5 shows predicted SmKS differential traveltimes as a function of epicentral distance for PREM with the lowermost-mantle and outer-core models described in section 2.4. While the modelled D″ structure has a stronger effect on the synthetic seismograms (Fig. 4) than low outermost-core velocities, Fig. 5 shows that the SmKS differential traveltimes are affected more strongly by KHOMC and EPOC-Vinet than by D″ structure. The ULVZ models with −10 per cent v_p and −30 per cent v_s result in approximately the same dt^{m-n} values as the −3 per cent D″ layer. Using a different 1-D reference earth model in D″ has hardly any effect on the differential traveltimes, as shown in Fig. 5 by the near-zero predictions for PREM with model AK135 in D″.

For comparison with data, we also show the seismic body-wave array measurements from Kaneshima & Helffrich (2013) in Fig. 5, of which only the Fiji measurements (KH2013_F) were used to create model KHOMC. The Argentina measurements (KH2013_A) and other measurements from Kaneshima & Helffrich (2013) at smaller distances (KH2013 rest) sample different mantle and core regions than the Fiji data, but they agree within their uncertainties with KHOMC predictions. Kaneshima & Helffrich (2013) also show that their outermost-core velocity model derived from the Argentina data is similar to KHOMC. Fig. 5 shows that the effect of a global D″ layer is insufficient to explain the differential traveltimes that have been attributed to low outermost-core velocities. The data from Alexandrakis & Eaton (2010), AE2010, with respect to PREM predictions are also shown in Fig. 5. The S4KS–S3KS data are obtained from their measurements by subtracting the S4KS-S2KS and the S3KS-S2KS measurements. All measurements result in positive dt^{3-2} and dt^{4-3} values and for the smaller distances the dt^{3-2} values are similar to the KHOMC predictions. These data appear not to be in conflict with the presence of low outermost-core velocities, meaning that the different outer-core velocities found by Alexandrakis & Eaton (2010) and for example Kaneshima & Helffrich (2013) are likely a consequence of the different modelling and interpretation methods. The AE2010 data unfortunately lack the distance range variation required to discriminate between models. Table 2 shows the average misfits for the model predictions shown Fig. 5 to the different data sets, which were calculated as

$$\chi = \sqrt{\frac{1}{N}\sum_{i=1}^{N}\left(\frac{d_i^{obs} - d_i^{syn}}{d_i^{obs}}\right)^2}, \qquad (5)$$

where N is the number of measurements, d_i^{obs} is the measurement and d_i^{syn} the model prediction.

The paths of SmKS waves (Fig. 1a) change significantly for increasing epicentral distance, sampling a larger section and larger depths of the core. For low outer-core velocities, this results in an increase of dt^{4-3} and dt^{5-3} over distance that is seen for both KHOMC and EPOC-Vinet. The effect of D″ structure on dt^{m-n} stays relatively constant for increasing distance, as there is a smaller effect of changing the paths through D″ for increasing epicentral distance on the differential traveltimes.

Model KHOMC is not only slower, it also has a steeper gradient in velocity than reference model PREM. We use the dt^{m-n} predictions for the outer-core layer with a constant reduction in v_p of −0.04 km s^{-1} (the dashed blue lines in Fig. 5), and therefore with the same gradient in velocity as PREM, to test the effect of the velocity gradient on SmKS differential traveltimes. For this model the dt^{4-3} and dt^{5-3} differential times are almost zero and even slightly negative. Differential traveltimes resulting from outer-core structure, as calculated with respect to differential traveltimes for the reference model, are therefore predominantly the result of the gradient in velocity with respect to the reference model. The velocity gradient of EPOC-Vinet is slightly less steep than KHOMC. This explains why differential traveltimes for KHOMC are often

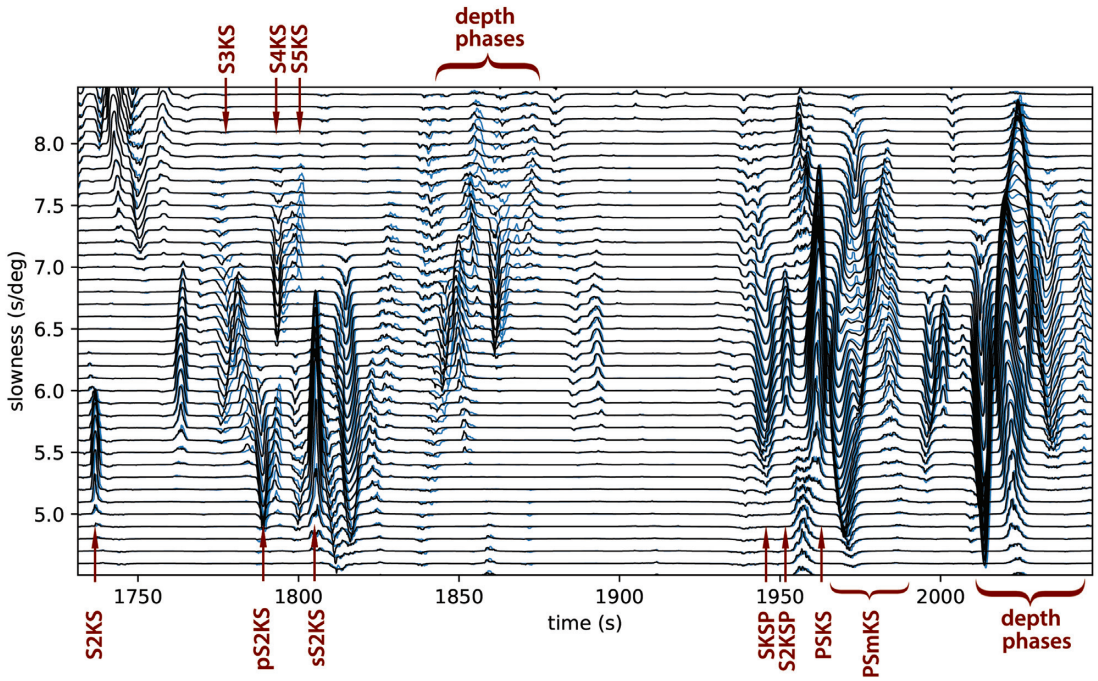

Figure 3. Radial-component vespagrams for synthetic reflectivity seismograms between 150° and 160°, with calculations for PREM in black and for PREM + KHOMC in blue. The used event depth is 150 km. The names of the phases are indicated in the figure.

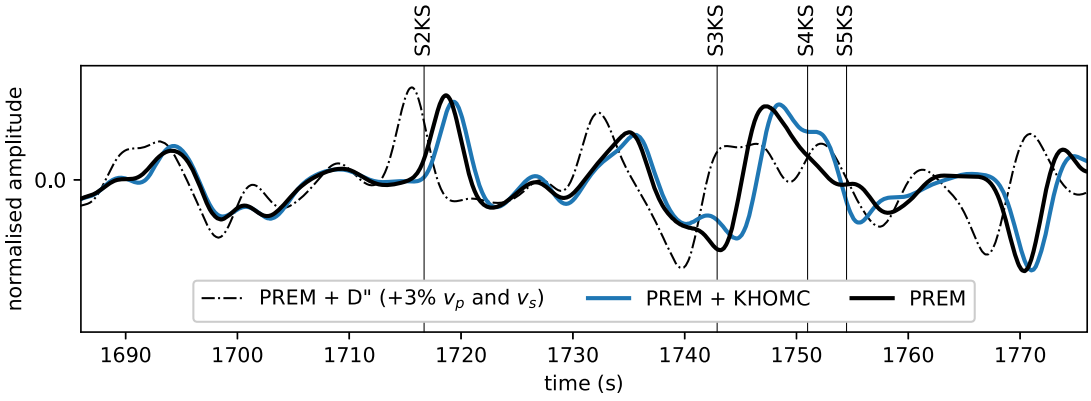

Figure 4. Radial-component reflectivity seismograms for PREM, PREM+KHOMC and PREM+D″ (280 km thick, +3 per cent for v_p and v_s). Predicted SmKS arrivals for PREM are also shown. The distance is 139.0° and the event depth is 150 km.

larger than for EPOC-Vinet, even though the velocity reduction of EPOC-Vinet is larger than that of KHOMC.

As opposed to the dt^{4-3} and dt^{5-3} predictions for the layer with a constant v_p reduction, dt^{3-2} does increase over distance. This increase in dt^{3-2} over distance is the result of the maximum depth of the low-velocity layer, which lies in between the maximum ray turning points of S3KS and S2KS for larger distances (the depth ranges sampled by the different SmKS phases are indicated by the vertical bars in Fig. 1). So for larger distances, S3KS is delayed by the low-velocity layer for its entire path in the outer core while S2KS is only partly affected. The maximum depth of KHOMC also lies in between the maximum ray turning points of S3KS and S2KS, but for KHOMC predictions dt^{3-2} decreases over distance. This is the result of the v_p perturbations of KHOMC with respect to PREM, which are nearly zero at these depths. EPOC-Vinet contains anomalous velocities throughout the entire outer core, resulting in an increase in dt^{3-2} over distance similar to dt^{4-3} and dt^{5-3}. Hence, as also noted by Kaneshima (2018), the trend in dt^{m-n} over distance may be used to constrain the maximum depth of anomalous outer-core velocities. As the Argentina data at larger distances indicate a decrease in dt^{3-2} with respect to the Fiji data at smaller distances, SmKS data indicate that low outer-core velocities likely do not extend to lower depths than where KHOMC reconciles with PREM. Kaneshima (2018) already concluded that based on their dt^{3-2} measurements, the thickness of the low-velocity outermost-core layer lies in between 300 and 450 km.

In summary, body-wave observations require a lower velocity than PREM in the outermost core, with a steeper velocity gradient than PREM, even when potential global D″-structure is taken into account. Observed differential traveltimes dt^{m-n} are explained better by KHOMC than by EPOC-Vinet, also indicating that a steeper velocity gradient than PREM is required. The depth-extent of low outermost-core velocities is constrained by dt^{3-2} at larger distances, measurements of which are better explained by KHOMC than by

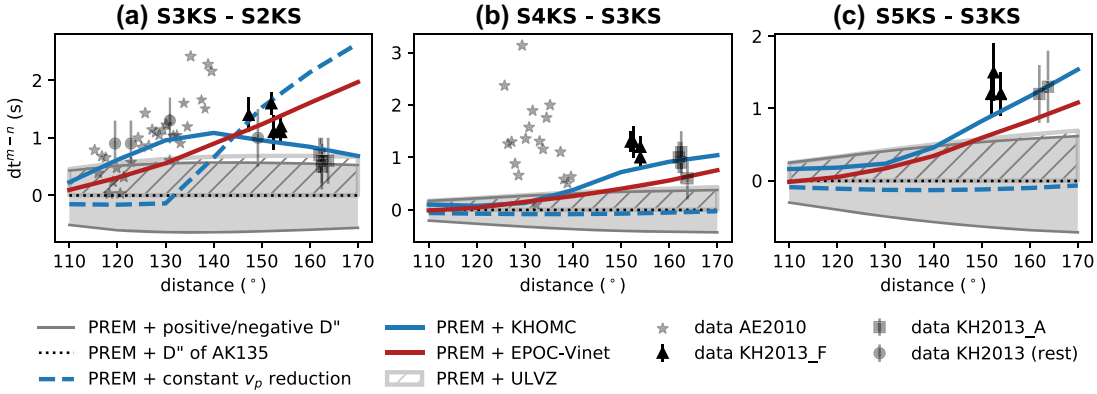

Figure 5. Predicted (ray-theoretical) SmKS differential traveltimes as a function of epicentral distance for several outer-core velocity models, for (a) S3KS–S2KS, (b) S4KS–S3KS and (c) S5KS–S3KS with respect to differential times for PREM. Predictions for PREM with AK135 in D″ are shown with a black dotted line. The upper grey line denotes predictions for PREM with a 280-km thick D″-layer with −3 per cent v_p and v_s; the lower grey line for a 280-km-thick D″-layer with +3 per cent v_p and v_s. The upper line of the grey hatched area shows predictions for a 40-km-thick ULVZ with −10 per cent v_p and −30 per cent v_s. Predictions for PREM with KHOMC in the outer core are in blue and predictions in red are for PREM with EPOC-Vinet in the outer core. Dashed blue lines indicate predictions for PREM with a 480-km-thick outermost-core layer with a constant reduction in velocity of –0.04 km s^{-1} with respect to PREM. AE2010 corresponds to the data from Alexandrakis & Eaton (2010), KH2013_F to the Fiji array measurements of Kaneshima & Helffrich (2013) that were used to create KHOMC, KH2013_A corresponds to the Argentina array measurements of Kaneshima & Helffrich (2013) and KH2013 (rest) to the remaining array measurements of Kaneshima & Helffrich (2013).

Table 2. Average misfit to data for SmKS differential traveltime predictions shown in Fig. 5 for several outer(most) core and D″ models. AE2010 corresponds to the data from Alexandrakis & Eaton (2010), KH2013_F to the Fiji array measurements of Kaneshima & Helffrich (2013) that were used to create KHOMC, KH2013_A corresponds to the Argentina array measurements of Kaneshima & Helffrich (2013) and KH2013 (rest) to the remaining array measurements of Kaneshima & Helffrich (2013).

Data set	KHOMC	EPOC-Vinet	D″ (−3 per cent v_p, −3 per cent v_s)	D″ (+3 per cent v_p, +3 per cent v_s)	ULVZ	D″ of AK135
AE2010 dt^{3-2}	6.013	2.871	5.110	5.842	5.628	1.018
AE2010 dt^{4-3}	0.819	0.833	0.845	1.525	0.852	1.004
KH2013_F dt^{3-2}	0.271	0.200	0.555	1.450	0.459	1.003
KH2013_F dt^{4-3}	0.342	0.615	0.705	1.296	0.674	1.003
KH2013_F dt^{5-3}	0.273	0.470	0.563	1.439	0.527	1.004
KH2013_A dt^{3-2}	0.383	1.905	0.136	1.925	0.209	1.007
KH2013_A dt^{4-3}	0.327	0.343	0.586	1.428	0.534	1.004
KH2013_A dt^{5-3}	0.029	0.280	0.526	1.474	0.476	1.004
KH2013 (rest) dt^{3-2}	0.230	0.537	0.468	1.538	0.395	1.004

EPOC-Vinet. It should be noted that variable D″ structure instead of a global layer may increase the differential traveltimes, but to model this effect is beyond the scope of this study.

3.2 Normal-mode centre frequencies

Irving *et al.* (2018) proposed model EPOC-Vinet to explain the measured centre frequencies of 319 normal modes as published by various studies (Masters & Widmer 1995; Resovsky & Ritzwoller 1998; Deuss *et al.* 2013; Koelemeijer *et al.* 2013). PREM was used for the 1-D structure in the rest of the Earth, so that the differences between the measured centre frequencies and the calculated PREM frequencies were fully attributed to outer-core structure. For 64 of these modes, the sensitivity kernels for v_p and density are shown in Fig. 6(a) and the measured centre-frequency shifts with respect to PREM are shown in Fig. 6(b). This selection of modes was made by Irving *et al.* (2018) and contains the modes that have at least 10 per cent of their sensitivity to velocity and density in the outer core. The bars show the uncertainties calculated by Irving *et al.* (2018) as the difference between calculated centre frequencies for PREM and for mantle model STW105 (Kustowski *et al.* 2008). These uncertainties therefore represent a relative measure for the effect of mantle structure on the data. Here, we show the predicted centre-frequency shifts for PREM with KHOMC and EPOC-Vinet in the outer core (Fig. 6b). We find that KHOMC overall improves the fit to the data compared to PREM, although the measured frequency shifts are still underestimated. EPOC-Vinet predicts larger frequency shifts, which approximate the data better for the majority of modes. The large spread seen in the data is also better predicted by EPOC-Vinet than by KHOMC. The misfits of the predictions for the different outer-core models and all other models used in this study, again calculated using eq. (5), are shown in Fig. 7.

The effect of outer-core models on normal-mode spectra is shown in Fig. 8. Synthetic spectra for modes ${}_{19}S_{11}$ and ${}_{17}S_{14}$, calculated for PREM and PREM with EPOC-Vinet, illustrate that radial perturbations in outer-core structure lead to frequency shifts that are easily observable in the normal-mode spectrum. Calculations for PREM with KHOMC show that the smaller velocity perturbations

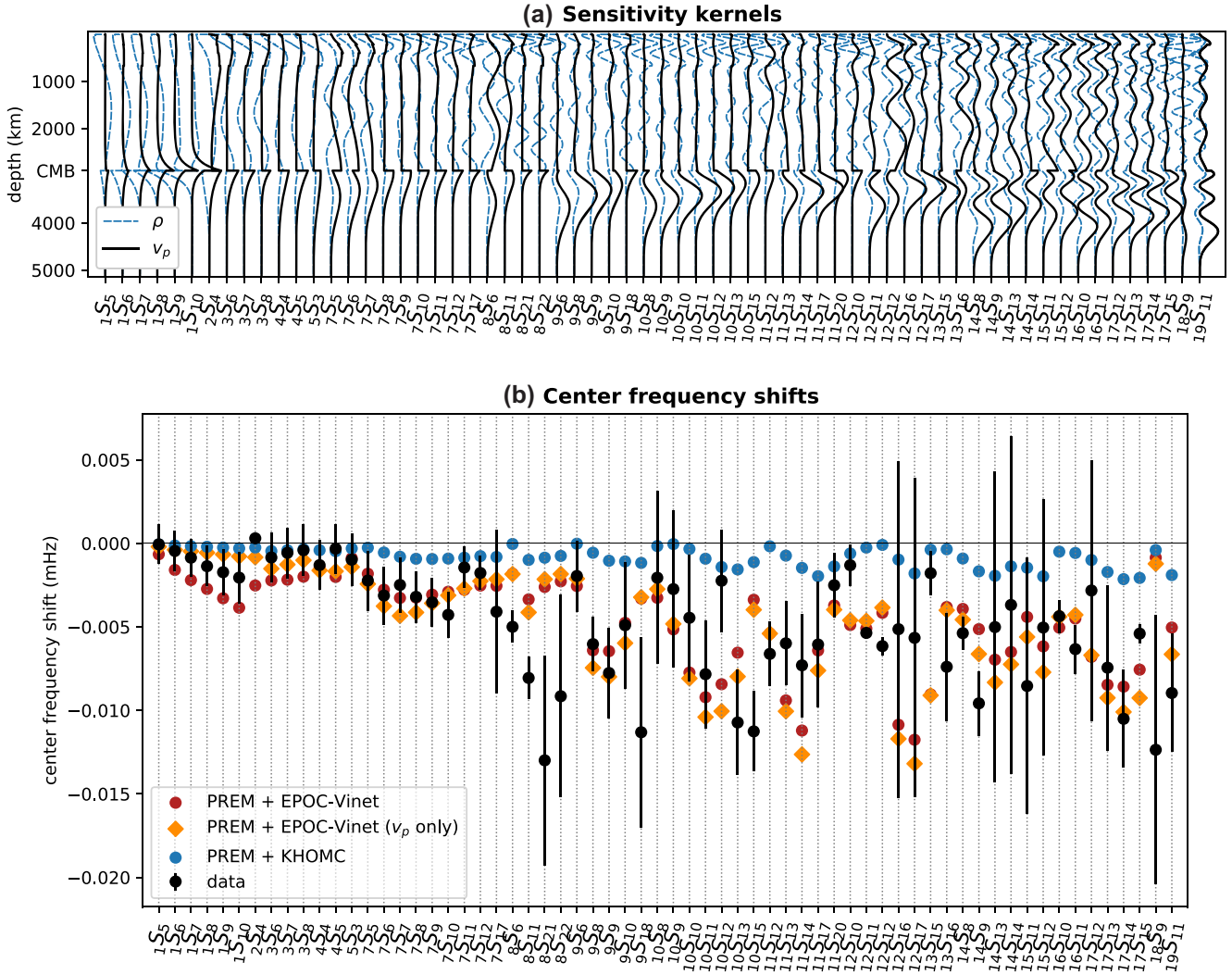

Figure 6. (a) Sensitivity kernels of outer-core sensitive normal modes. (b) Centre frequency shifts with respect to PREM frequencies as measured by various studies (black circles) and as predicted for outer-core models KHOMC, EPOC-Vinet and the velocity model of EPOC-Vinet alone. These normal modes are a selection of the most outer-core sensitive modes that were used by Irving *et al.* (2018) to create EPOC-Vinet.

of KHOMC lead to barely observable changes to the normal-mode spectrum.

Irving *et al.* (2018) excluded specific modes from their calculations for which they expected the centre-frequency measurements to be affected by strong cross-coupling. This concerns also Stoneley modes, normal modes that form at the core–mantle boundary and the inner-core boundary. CMB Stoneley modes are strongly coupled to other modes through 3-D structure near the core–mantle boundary. Since cross-coupling was included in the measurements of Koelemeijer *et al.* (2013), their measured centre-frequency perturbations have been corrected for the potential effects of heterogeneous D″ structure. Stoneley modes are of particular interest to us, due to their strong sensitivity to velocity and density in the outermost core (Fig. 9a). We have calculated centre-frequency shifts (Fig. 9b) using the different outer-core models for a selection of first overtones (${}_1S_5 - {}_1S_{10}$) that were used to create EPOC-Vinet and added the Stoneley modes (${}_1S_{11} - {}_3S_{26}$). Also shown are the measured Stoneley-mode centre frequencies from Koelemeijer *et al.* (2013), which follow a similar trend as predicted for the outer-core models. We therefore suggest that the frequency shifts of Stoneley-mode measurements with respect to PREM are predominantly the result of changes in radial Earth structure, especially in the outer core, rather than some arbitrary effect from cross-coupling that was unaccounted for in the measurements of these modes.

For the modes in Fig. 9(b), KHOMC-predictions generally underestimate and predictions for EPOC-Vinet overestimate the centre-frequency shifts of the measurements. KHOMC overall provides a better fit to the data than EPOC-Vinet, as also shown by the misfit calculations in Fig. 7. The trend in frequency shifts for the different modes, as seen both for KHOMC and EPOC-Vinet predictions and for most of the data, correspond to the relative strength of the simple v_p and ρ kernels in the outermost core (Fig. 9a).

3.2.1 *Density*

The centre frequencies of Stoneley modes are nearly twice as sensitive to density as they are to velocity in the outermost core, as shown by the sensitivity kernels in Fig. 9(a). Both negative perturbations in v_p and positive perturbations in ρ result in negative frequency

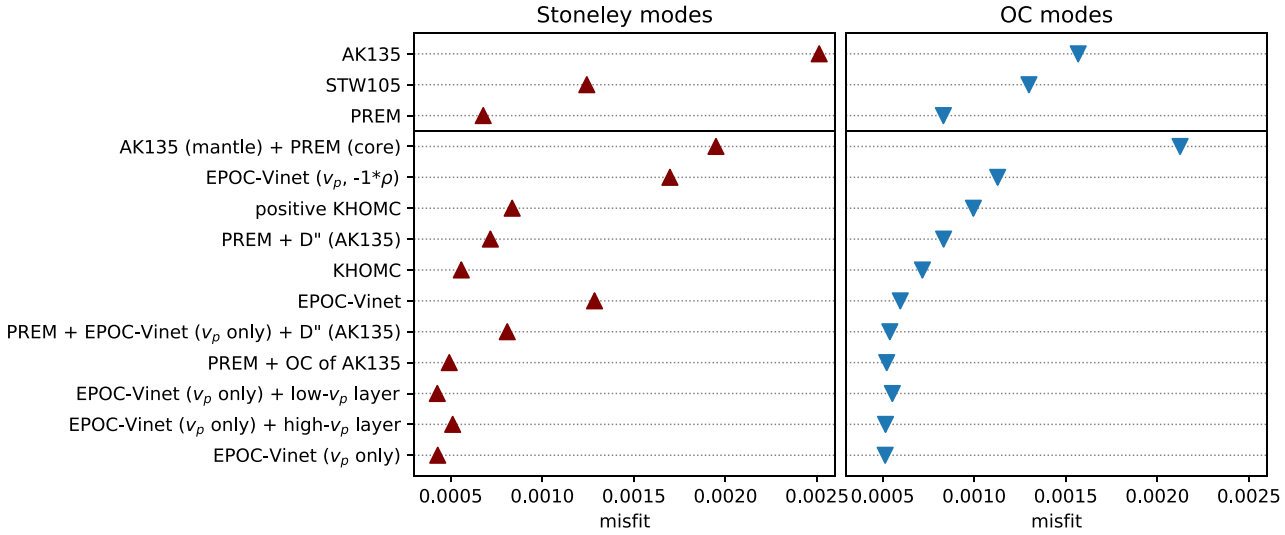

Figure 7. Misfit to normal-mode centre frequency measurements for the modelling discussed in this study. For the outer-core models PREM was used in the mantle, unless indicated otherwise.

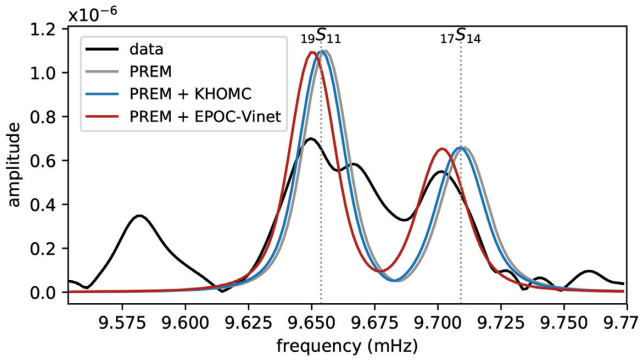

Figure 8. Vertical-component spectra at station ARU for the 9 June 1994 Bolivia earthquake. Synthetic spectra are calculated for modes $_{19}S_{11}$ and $_{17}S_{14}$, using 1-D models PREM, PREM with KHOMC and PREM with EPOC-Vinet in the outer core. These calculations do not consider the effects of Earth's rotation and 3-D structure, which means that the shapes and amplitudes of the peaks in the data are not approximated by the synthetics.

shifts, due to the signs of the kernels in the outer core. Centre-frequency calculations for EPOC-Vinet's velocity model alone, using the outer-core density profile of PREM, are shown in Figs 6(b) and 9(b). Apart from the first, second and third overtones ($_1S_5$ – $_3S_8$), the frequencies of the modes used to create EPOC-Vinet show only minor differences between calculations with and without EPOC-Vinet's density model. On the other hand, using only the velocity model of EPOC-Vinet greatly reduces the frequency shifts of Stoneley modes with respect to PREM. Stoneley modes are therefore an effective means to study the density structure directly below the core–mantle boundary.

The predictions for EPOC-Vinet's velocity model approximate the Stoneley-mode data better than predictions for KHOMC and full EPOC-Vinet (Fig. 9b), although the frequency shifts of the data are now underestimated. Assuming EPOC-Vinet velocities in the outer core, these predictions show that the centre frequencies of Stoneley modes require an outermost-core density that is higher than PREM, but lower than EPOC-Vinet. Predictions for EPOC-Vinet where the sign of the density perturbations with respect to PREM is flipped (Fig. 9b) show a trend that is opposite to the data, implying that low-velocity, low-density stratification is not immediately supported by the Stoneley-mode data when PREM is used as the reference model. It is interesting to note that the centre frequencies of the outer-core sensitive modes used to create EPOC-Vinet are also better approximated when only the velocity model is changed from PREM to EPOC-Vinet, instead of both the velocity and density model. This is shown by the calculated misfits in Fig. 7.

3.2.2 D″ structure

Any trade-off between D″ structure and outermost-core structure on the centre frequencies of normal modes is limited to the effect of radial structure. Predicted centre frequency shifts for PREM with the velocities and densities of AK135 in D″ (150 km thick) are shown in Fig. 10 and the corresponding misfits again in Fig. 7. For the Stoneley modes (Fig. 10a), these predictions are very similar to the calculations for EPOC-Vinet's velocity model. In fact, predictions for PREM with the D″ structure from AK135 and the outer-core structure from EPOC-Vinet's velocity model approximate most of the data quite well, reducing the need for a higher outer-core density based on the measurements. As a result of their similar sensitivity kernels in D″ (Fig. 9a), the D″ structure of AK135 has a similar effect on the Stoneley-mode predictions. This is not the case for the outer-core sensitive modes (Fig. 9b), where the D″ of AK135 leads to an increase in centre frequency for about a third of the modes and a decrease for the rest of the modes. This inconsistent effect from mode to mode means that it is difficult to explain the predominantly negative frequency shifts seen in the data as the result of radial D″ structure alone, even though the effect of D″ structure on the centre frequencies is substantial. Thus, deviations from the reference model in D″ have a notable effect on the centre frequencies and may affect the outermost-core velocity and density required by centre-frequency measurements, but the modelled radial D″ structure is insufficient to fully explain the data.

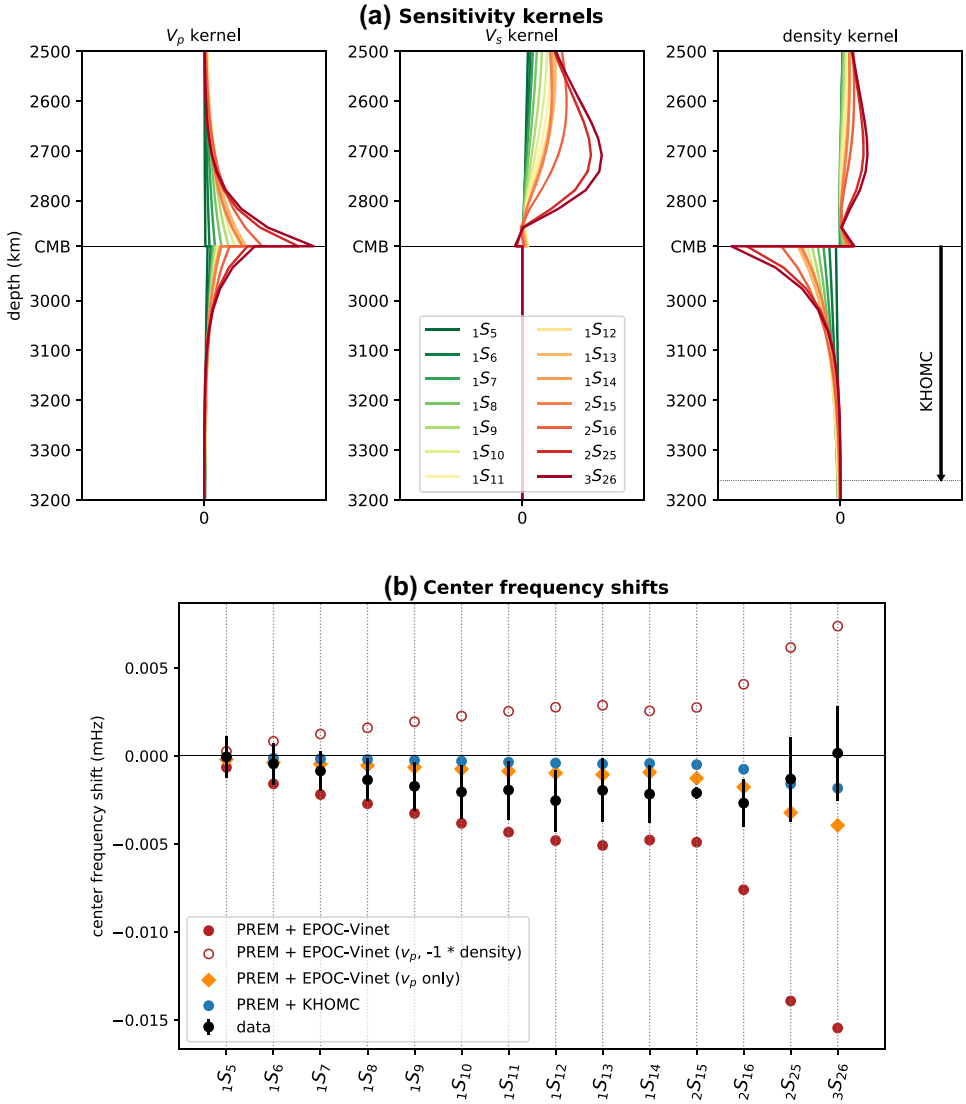

Figure 9. (a) Sensitivity kernels (v_p, v_s and ρ) of Stoneley modes ($_1S_{11} - {}_3S_{26}$) and a selection of first overtones ($_1S_5 - {}_1S_{10}$) for the region at the bottom of the mantle and the top of the outer core. The depth-extent of model KHOMC is shown for comparison. (b) Centre frequency shifts of the Stoneley modes and first overtones with respect to PREM frequencies, as predicted for outer-core models KHOMC, EPOC-Vinet and the velocity model of EPOC-Vinet alone. Also shown are the Stoneley-mode measurements from Koelemeijer *et al.* (2013) and the measured first overtones also shown in Fig. 6(a).

4 DISCUSSION

4.1 Reconciling body-wave and normal-mode data

The long periods of normal-mode oscillations limit their resolution to long-wavelength Earth structure only, meaning that the presence of a radial stratified layer in the outermost core is unlikely to be irrefutably proven or contradicted by normal-mode data. However, the insensitivity of normal-mode centre frequencies to 3-D structure and their direct sensitivity to density provide complementary information to body-wave data. Hence, our aim is to evaluate the constraints on outer-core properties provided by the combination of measurements of SmKS differential traveltimes and of the centre frequencies of normal modes.

First, we assess the constraints of the combined data on the outer-core's velocity profile, which should explain both the differential traveltimes of SmKS waves and the centre frequencies of outer-core sensitive normal modes that have very little sensitivity to density (i.e. the modes in Fig. 6b where predictions for EPOC-Vinet and for the velocity model of EPOC-Vinet alone are similar). SmKS differential traveltimes constrain the gradient in velocity and the depth-extent of low outermost-core velocities, while normal-mode centre frequencies provide information on absolute velocity and density. We have shown that SmKS differential traveltimes require a velocity gradient in the outermost core that is steeper than EPOC-Vinet and similar to KHOMC. The measurements of dt^{3-2} at large epicentral distances [e.g. measurements for the Argentina event by Kaneshima & Helffrich (2013), as shown in Fig. 5a], which constrain the maximum depth-extent of low outermost-core velocities, are also explained better by KHOMC than by EPOC-Vinet. This maximum depth-extent is limited to 300–450 km below the CMB by Kaneshima (2018). Normal-mode centre-frequency measurements (Fig. 6b) require low-velocity perturbations that are stronger than KHOMC and similar to EPOC-Vinet. Based on these combined observations, a suitable velocity model of the outermost core

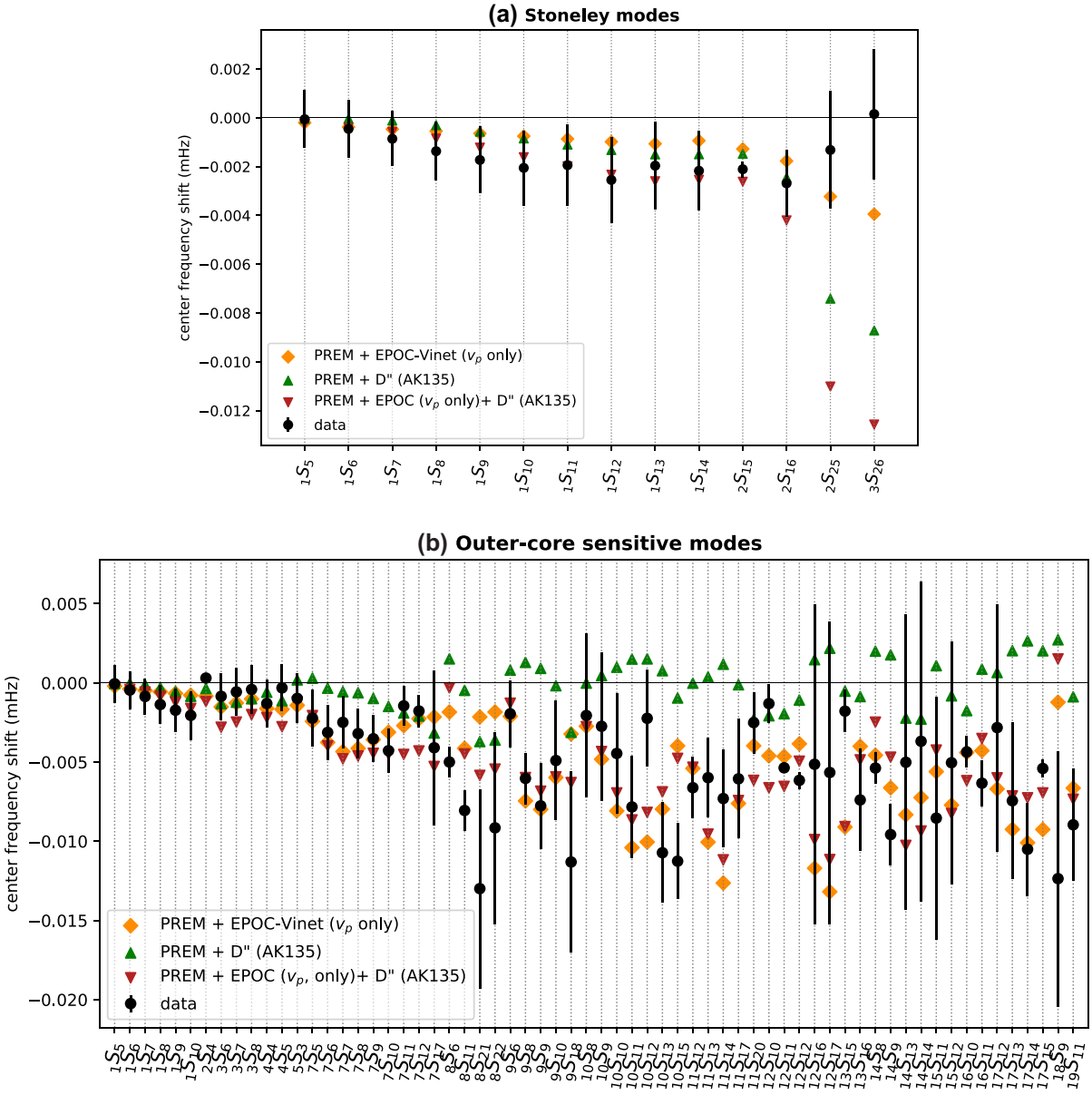

Figure 10. Centre frequency shifts with respect to PREM frequencies for (a) Stoneley modes and first overtones and (b) outer-core sensitive modes. Predictions are shown for PREM with EPOC-Vinet's velocity model in the outer core, for PREM with the D″ of AK135 and for PREM with EPOC-Vinet's velocity model in the outer core and the D″ of AK135. Additional data in (a) are from Koelemeijer *et al.* (2013), data in (b) have been assembled by Irving *et al.* (2018) from various studies.

would (1) contain velocity perturbations that are similar to EPOC-Vinet and (2) decrease in strength with a KHOMC-like gradient to (3) a maximum depth of 300–450 km below the CMB. However, connecting (1) and (3) results in a velocity gradient that is steeper than KHOMC, which would result in larger SmKS differential traveltimes. Figs S4 and S5 contain calculated SmKS differential times and normal-mode centre frequencies for an estimated model (Fig. S3) that forms a compromise between the outer-core velocity profiles required by both data types. This estimated model is more similar to KHOMC than to EPOC-Vinet and predictions for this model therefore approximate the SmKS data reasonably well, although dt^{3-2} is now overestimated for larger distances. The centre-frequency predictions are very similar to KHOMC, meaning that the negative shifts in centre frequency are not strong enough to explain the normal-mode data. A model that contains lower outermost-core velocities will improve the centre-frequency predictions but the resulting steeper velocity gradient or larger depth-extent of low velocities will reduce the fit to the measured SmKS differential times. This implies that the body-wave and normal-mode observations of the outermost core are not readily reconciled by a given velocity profile and that effects of other Earth structure are also present in measured SmKS differential traveltimes or normal-mode centre frequencies, or both.

The velocity and density profiles of EPOC-Vinet should not be considered independently, as they have been derived from obeying a single equation of state in the outer core. However, the normal modes from which EPOC-Vinet was derived are far more sensitive to velocity than to density. This means that regardless of the density profile, the velocity profile required by these modes will be very similar. We therefore consider the Stoneley-mode predictions for the

velocity model of EPOC-Vinet a reliable indication that Stoneley modes require a density in the outermost core that is higher than PREM, but lower than EPOC-Vinet. As shown in Fig. 10(a), using a different reference model (AK135) in D″ reduces the need for a higher outer-core density to explain measured Stoneley-mode centre frequencies even further. Irving *et al.* (2018) show that the density profile of EPOC-Vinet leads to an overestimation of the Earth's mass and moment of inertia, which means that using lower densities than EPOC-Vinet may result in a more physically feasible model of the outer core.

Outer-core structure and D″ structure trade off both for SmKS differential traveltimes and for normal-mode centre frequencies. SmKS differential traveltimes are only affected by potential strong lateral variations in D″ velocity, as represented by the modelled ±3 per cent D″ layer, while they are practically unaffected by the smaller variations resulting from changing the 1-D reference model in D″. On the other hand, the centre frequencies of normal modes are insensitive to 3-D structure but are substantially affected by changing the 1-D reference model in D″. The observed positive dt^{m-n} values and negative centre-frequency shifts therefore cannot be produced by the same trade-off and the most straightforward explanation for the measurements of both positive dt^{m-n} values and negative centre-frequency shifts is a low-velocity outermost core. Moreover, our modelled D″ structure fails to explain the observations for either data type we use here. Differential traveltimes measured for vastly different source–receiver geometries can be explained by the same low outermost-core velocities of KHOMC (Kaneshima & Helffrich 2013; Kaneshima & Matsuzawa 2015; Kaneshima 2018), which strongly suggests that these differential traveltimes are the result of global outermost-core structure instead of heterogeneous lower-mantle structure.

Until now, we have neglected that changes in the depth of the core–mantle boundary will also have an effect on SmKS differential traveltimes and the centre frequencies of normal modes. A change in CMB depth cannot explain the measurements of either data type (see Figs S6 and S7).

4.2 The choice of reference model

So far we have only considered anomalous outer-core velocity and density structure with respect to PREM, meaning that we can only comment on the agreement of seismic data with the presence of stratification in an outer core otherwise described by PREM. Other reference models may be considered, although the choice is limited by the fact that both a density model and an attenuation model are required to calculate normal-mode centre frequencies that can be compared to the measurements. Alternatives are STW105 (Kustowski *et al.* 2008) and AK135 (Kennett *et al.* 1995) with the attenuation model of AK135-F (Montagner & Kennett 1996), both of which result in a worse fit to the normal-mode data than PREM (Fig. 7). For both models this poor fit to the measured centre frequencies is the result of mantle structure. For STW105 this is immediately obvious, as the STW105 core is identical to PREM and any difference in misfit therefore is the result of mantle structure. For AK135 this is shown in Fig. 7 by the predictions for PREM in the core with AK135 in the mantle, which result in a poorer fit to the data than predictions for just PREM, and predictions for AK135 in the core and PREM in the mantle, which fit the data better than the PREM predictions. Using STW105 or AK135 as the reference model would then lead us to interpret known mantle effects as the result of outer-core structure. In addition, since KHOMC and EPOC-Vinet were both inferred using PREM as a reference model in the rest of the Earth, using any other reference model in the mantle would again result in the interpretation of the misfit caused by mantle structure as required deviations from the reference model in the outer core. The potential effect of mantle structure on the centre frequencies is included in our modelling by calculating the uncertainties as described in Section 3.2.

Another factor for the choice of reference model is that the velocity and density structure of the outer core can only provide information on the presence of stratification when considered with respect to a model that corresponds to a well-mixed, homogeneous outer core—that is follows an adiabatic gradient—which AK135 does not. Therefore, deviations in velocity and density considered with respect to AK135 contain no information regarding the presence of stratification. It is possible to consider the presence of stratification with respect to EPOC-Vinet, as its velocity and density profiles correspond to an equation of state. SmKS differential traveltime predictions for high and low-velocity layers with respect to EPOC-Vinet, now using PREM + EPOC-Vinet as the reference model instead of PREM, are shown in Fig. 11. These high and low-velocity layers with respect to EPOC-Vinet were made by respectively adding to or subtracting from the velocity model of EPOC-Vinet the absolute difference between KHOMC and PREM. The array measurements from Kaneshima & Helffrich (2013) are now also shown with respect to PREM + EPOC-Vinet. The dt^{4-3} and dt^{5-3} measurements, even though they are smaller than when calculated with respect to PREM, indicate that low velocities are still required when EPOC-Vinet is used as the reference model. The dt^{3-2} measurements however, when considered with respect to EPOC-Vinet, show that for smaller distances (i.e. shallower depths in the outer core) low velocities with respect to EPOC-Vinet are required, while at larger distances (i.e. at larger depth in the outer core), velocities should be higher than EPOC-Vinet. Since lowermost-mantle structure may also affect these differential traveltimes, the need for anomalous velocities in the outermost core is less robust than when PREM is used as the reference model. The misfit to the Stoneley-mode measurements is also lower for calculations for the velocity model of EPOC-Vinet with a low-velocity layer (Fig. 7), but for the outer-core sensitive modes the misfit increases for a low-velocity layer and decreases for a high-velocity layer with respect to EPOC-Vinet.

4.3 Do seismic data require stratification of the outermost core?

We can now state with more certainty that seismological data require a low-velocity outermost core with respect to PREM. It remains difficult to explain these low velocities as the result of a stratified layer at the top of the outer core, considering that the different studies on the formation of stratification (Table 1) often predict a seismically fast outermost core. Predicted SmKS differential traveltimes and shifts in normal-mode centre frequencies resulting from a positive outermost-core velocity with respect to PREM are shown in Figs 12(a) and (b), respectively. The SmKS differential traveltimes for fast outer-core velocities are negative with respect to the predictions for PREM. Even when the differential traveltimes of a D″-layer with negative velocities (−3 per cent, upper grey line in Figs 12a–c) would be added, the resulting differential traveltimes remain mostly negative with respect to the PREM predictions. The change of dt^{m-n} over distance predicted for positive KHOMC is also opposite to the predictions for regular KHOMC. As already shown in Fig. 11, a

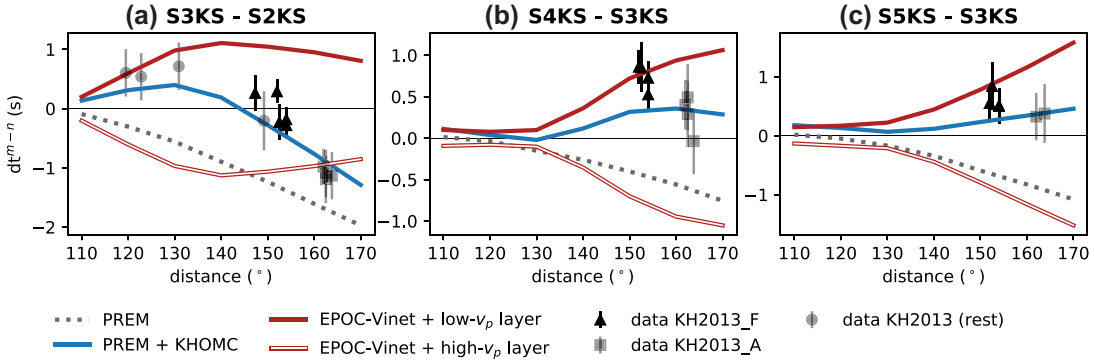

Figure 11. SmKS differential traveltimes with respect to calculations for EPOC-Vinet as a function of distance. Predictions are shown for low and high-velocity layers with respect to EPOC-Vinet, where the strength of velocity perturbations is equal to the absolute difference between KHOMC and PREM. Predictions for PREM and KHOMC are also shown, as well as the array measurements from Kaneshima & Helffrich (2013).

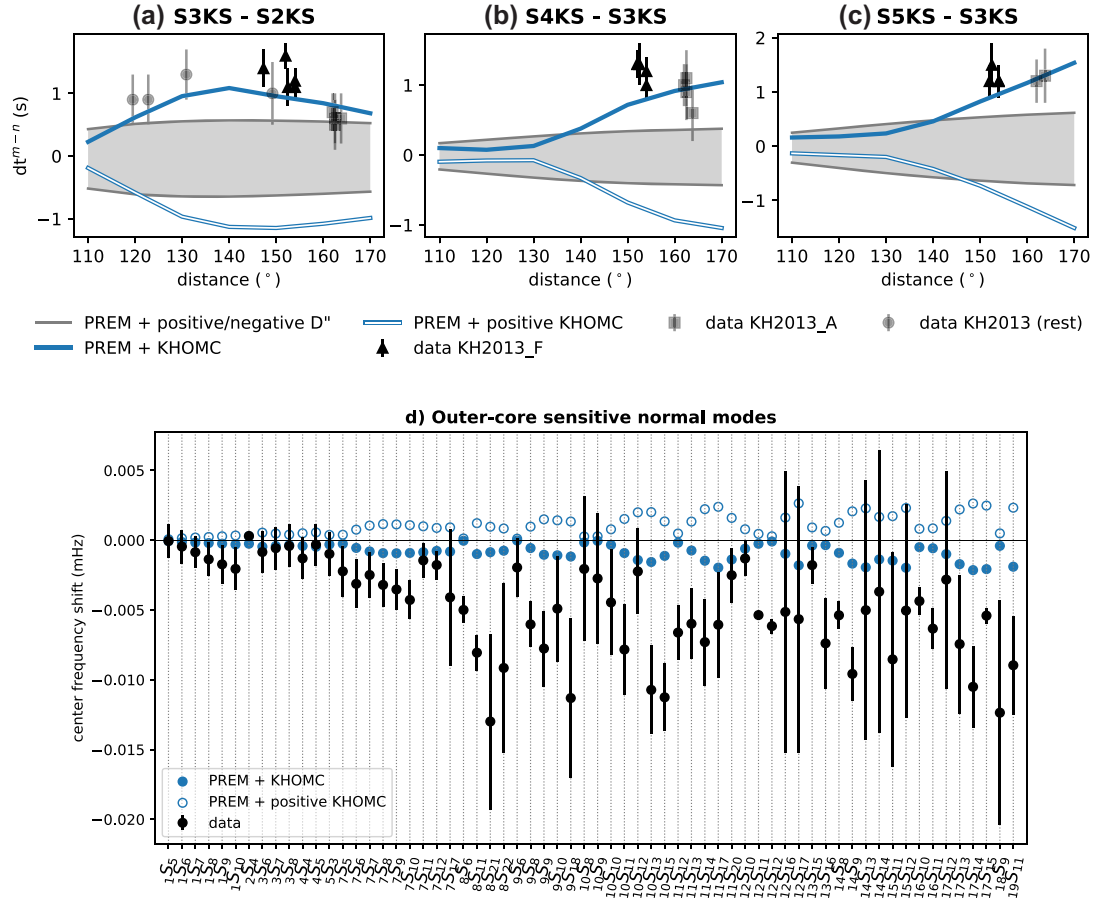

Figure 12. (a–c) SmKS differential traveltimes with respect to calculations for PREM as a function of distance. Predictions are shown for KHOMC and for KHOMC with velocity perturbations of opposite sign. Upper grey line: dt for a 280-km-thick D$''$-layer with −3 per cent v_p and v_s. Lower grey line: +3 per cent v_p and v_s. Data are from Kaneshima & Helffrich (2013). (d) Centre frequency shifts with respect to PREM frequencies for outer-core sensitive modes, again showing predictions for KHOMC and for KHOMC with velocity perturbations of opposite sign. Data have been assembled by Irving *et al.* (2018) from various studies.

high-velocity layer with respect to EPOC-Vinet is also not supported by SmKS differential traveltime measurements. Fig. 12(d) shows that the shifts in normal-mode centre frequencies will be positive for increased velocities with respect to PREM in the outermost core. The trend in frequency shifts per normal-mode overtone branch is the exact opposite as for regular KHOMC.

Thus, both SmKS differential traveltime observations and measured shifts in the centre frequencies of normal modes contradict the presence of high-velocity outermost-core material with respect to PREM. These results rule out the processes in Table 1 that produce such stratification as the dominant source of the observed variations in outermost-core velocity when PREM is used as the reference

model. Assuming ideal mixing, this concerns barodiffusion (Gubbins & Davies 2013), an oxygen-enrichment of the outermost core due to core–mantle interactions (Buffett & Seagle 2010) and possibly also Fe–Si–O immiscibility (Arveson *et al.* 2019). The existence of thermal stratification in the outermost core is proposed by several recent studies (Davies *et al.* 2015; Buffett *et al.* 2016; Olson *et al.* 2018; Mound *et al.* 2019). None of these studies constrain seismic velocity in the stratified regions, although the effect of temperature on velocity in liquid iron has been shown to be rather small as a result of the small temperature dependence of the bulk modulus (Ichikawa *et al.* 2014). Low-density thermal stratification would then imply an increase, however small, in seismic velocity and would therefore be inconsistent with seismological observations. We do not exclude the existence of a thermally stratified outermost core, although thermal stratification alone likely cannot produce the observed seismic wave speeds. Even when considered with respect to the velocity model of EPOC-Vinet, high outermost-core velocities cannot explain SmKS differential traveltime measurements. High-velocity stratification with respect to the currently available velocity models of the outer core that represent a well-mixed, homogeneous outer-core composition is therefore not immediately supported by seismic data.

The remaining scenarios in Table 1 (Helffrich 2012; Brodholt & Badro 2017, Badro *et al*. 2014) may be responsible for the generation of stratification in the outermost core that is consistent with the observed low seismic velocity with respect to PREM. According to Brodholt & Badro (2017), the most feasible process for the generation of low-velocity compositional stratification in case of ideal mixing is the exchange of Si from the core with O from a partially molten lowermost mantle in the past. A former, partially molten lowermost mantle is supported by the high core heat-budget estimates of Davies *et al.* (2015). In case of non-ideal mixing as described by Helffrich (2012), low-velocity material at the top of the outer core may have accumulated after mixing with the core of an impactor in the early stages of Earth differentiation (Helffrich 2014). They also argue that other processes, such as barodiffusion, may in fact result in low velocities when non-ideal mixing is assumed.

Both thermal and compositional stratification of liquid outermost-core material need a lower density than the underlying material in order to be dynamically stable, while we have shown that the centre frequencies of Stoneley modes require a density that is higher than PREM but lower than EPOC-Vinet. The most straightforward interpretation of this result is therefore similar to Irving *et al.* (2018), namely that the velocity and density profiles in the outer core result from the self-compression of homogeneous outer-core material. However, we have shown that using a different reference model (AK135) in D″ reduces the need for a higher outer-core density to explain most measured Stoneley-mode centre frequencies (Fig. 10). The low outermost-core density expected for a stratified layer is nevertheless not directly supported by the Stoneley-mode measurements, since a low density again shifts the centre frequencies away from the measurements.

So far we have left the expected thickness of stratification out of consideration in the evaluation of the scenarios in Table 1, but it is important to note that estimates of layer thicknesses that can be produced by processes forming compositional stratification are significantly lower than the depth-extent of low velocity perturbations required by SmKS differential traveltimes (Kaneshima & Matsuzawa 2015). Helffrich (2014) find that only the scenario where the Earth's core mixes with that of an impactor may result in a present-day layer of sufficient thickness. They find that barodiffusion, in case of non-ideal mixing, is less likely to produce sufficiently thick stratification due to the expected low light-element diffusvities in the outer core.

Another concern regarding the presence of stratification (thermal or compositional) in the outermost core comes from variations in the magnetic field. While some variations of the magnetic field in time (∼60 yr) are more readily explained by a stratified outermost core due to the generation of MAC waves (Buffett *et al.* 2016), Gastine *et al.* (2019) show that, as a result of the lack of radial motion inside the stratified layer, small-scale features of the magnetic field would be smoothed out in the presence of stable stratification.

The presence of a very thin (∼5 km), solid and seismically fast stratified layer directly below the CMB has been proposed by Buffett *et al.* (2000). This stratification, consisting of an accumulated silicate phase, would be formed by the precipitation of light elements from the liquid core in order to restore chemical equilibrium with the mantle as the inner core grows. A fast, solid stratified layer with an estimated thickness of 2–12 km may also form as a result of Fe–O–S immiscibility (Helffrich & Kaneshima 2004), which may develop as a result of the enrichment of the outer core in light elements expelled by inner-core solidification. While the modelling of a thin high-velocity layer improves the synthetic reflectivity seismograms of Eaton & Kendall (2006), no evidence for the existence of such a layer is found using P4KP precursors (Helffrich & Kaneshima 2004) or S6KS arrival times (Kaneshima & Helffrich 2013). As this layer would be too thin to observe properly with SmKS differential traveltimes for $m \leq 5$ or normal-mode centre frequencies, we have not explored this scenario further here.

5 CONCLUSIONS

We have shown that both seismological body-wave and normal-mode observations require a low-velocity outermost core with respect to PREM, as well as a steeper velocity gradient than PREM, since the effects of D″ structure are insufficient to explain either the observations of SmKS differential traveltimes or the centre frequencies of normal modes sensitive to the outer core. These observations confirm that, if present, the formation of compositional stratification in the outermost core by means of an enrichment in light elements would require a process that produces low-velocity stratification. Stratification with high velocity, as a predicted from straightforward stratification-forming processes, is thus contradicted by our results. The centre frequencies of Stoneley modes provide complementary information on density and velocity directly below the core–mantle boundary. They also require low velocities at the top of the outer core and in addition show that the outermost-core density is higher than PREM but that the density in normal-mode based model EPOC-Vinet is too high. Stoneley modes therefore do not support the presence of buoyant stratification with respect to PREM in the outermost outer core.

ACKNOWLEDGEMENTS

We thank Sanne Cottaar and an anonymous reviewer for their helpful comments. RvT and AD were supported by the European Research Council (ERC) under the European Union's Horizon 2020 research and innovation programme (grant agreement No. 681535 - ATUNE) and a Vici award number 016.160.310/526 from the Netherlands organization for scientific research (NWO). SK was supported by MEXT/JSPS KAKENHI Grant No. 15H05832.

REFERENCES

Alexandrakis, C. & Eaton, D.W., 2010. Precise seismic–wave velocity atop Earth's core: no evidence for outer–core stratification, *Phys. Earth planet. Inter.,* **180**(1–2), 59–65.

Arveson, S.M., Deng, J., Karki, B.B. & Lee, K.K.M., 2019. Evidence for Fe-Si-O liquid immiscibility at deep Earth pressures, *Proc. Natl. Acad. Sci.,* **116**(21), 10 238–10 243.

Badro, J., Côté, A.S. & Brodholt, J.P., 2014. A seismologically consistent compositional model of Earth's core, *Proc. Natl. Acad. Sci.,* **111**(21), 7542–7545.

Birch, F., 1952. Elasticity and constitution of the Earth's interior, *J. geophys. Res.,* **57**(2), 227–286.

Brodholt, J. & Badro, J., 2017. Composition of the low seismic velocity E' layer at the top of Earth's core, *Geophys. Res. Lett.,* **44**(16), 8303–8310.

Buffett, B.A., Garnero, E.J. & Jeanloz, R., 2000. Sediments at the top of Earth's core, *Science,* **290**(5495), 1338–1342.

Buffett, B.A. & Seagle, C.T., 2010. Stratification of the top of the core due to chemical interactions with the mantle, *J. geophys. Res.,* **115**(B4), doi:10.1029/2009JB006751.

Buffett, B.A., Nicholas, K. & Holme, R., 2016. Evidence for MAC waves at the top of Earth's core and implications for variations in length of day, *J. geophys. Int.,* **204**(3), 1789–1800.

Bullen, K. E., 1950. An Earth model based on a compressibility–pressure hypothesis, *J. geophys. Int.,* **6,** 50–59.

Cobden, L., Thomas, C. & Trampert, J., 2015. Seismic detection of post-perovskite inside the Earth, in *The Earth's Heterogeneous Mantle: A Geophysical, Geodynamical, and Geochemical Perspective*, pp. 391–440, eds A. Khan & F. Deschamps, Springer.

Davies, C., Pozzo, M., Gubbins, D. & Alfé, D., 2015. Constraints from material properties on the dynamics and evolution of Earth's core, *Nat. Geosci.,* **8**(9), 678.

Deuss, A. & Woodhouse, J.H., 2001. Theoretical free–oscillation spectra: the importance of wide band coupling, *J. geophys. Int.,* **146**(3), 833–842.

Deuss, A., Ritsema, J. & van Heijst, H., 2013. A new catalogue of normal–mode splitting function measurements up to 10 mHz, *J. geophys. Int.,* **193**(2), 920–937.

Dziewonski, A.M. & Anderson, D.L., 1981. Preliminary Reference Earth Model, *Phys. Earth planet. Inter.,* **24**(4), 297–356.

Eaton, D.W. & Kendall, J.M., 2006. Improving seismic resolution of outermost core structure by multichannel analysis and deconvolution of broadband SmKS phases, *Phys. Earth planet. Inter.,* **155**(1–2), 104–119.

Gastine, T., Aubert, J. & Fournier, A., 2019. Dynamo-based limit to the extent of a stable layer atop Earth's core, *Geophys. J. Int.,* **200,** 1–17.

Garnero, E.J., Helmberger, D.V. & Grand, S.P., 1993. Constraining outermost core velocity with SmKS waves, *Geophys. Res. Lett.,* **20**(22), 2463–2466.

Garnero, E.J., 2000. Heterogeneity of the lowermost mantle, *Ann. Rev. Earth planet. Sci.,* **28**(1), 509–537.

Giardini, D., Li, X. D. & Woodhouse, J.H., 1988. Splitting functions of long-period normal modes of the Earth, *J. geophys. Res.,* **93**(B11), 13 716–13 742.

Gubbins, D. & Davies, C.J., 2013. The stratified layer at the core–mantle boundary caused by barodiffusion of oxygen, sulphur and silicon, *Phys. Earth planet. Inter.,* **215,** 21–28.

Hales, A.L. & Roberts, J.L., 1971. The velocities in the outer core, *Bull. seism. Soc. Am.,* **61**(4), 1051–1059.

Helffrich, G., 2012. How light element addition can lower core liquid wave speeds, *J. geophys. Int.,* **188,** 1065–1070.

Helffrich, G., 2014. Outer core compositional layering and constraints on core liquid transport properties, *Earth planet. Sci. Lett.,* **391,** 256–262.

Helffrich, G. & Kaneshima, S., 2004. Seismological constraints on core composition from Fe–OS liquid immiscibility, *Science,* **306**(5705), 2239–2242.

Helffrich, G. & Kaneshima, S., 2010. Outer–core compositional stratification from observed core wave speed profiles, *Nature,* **468**(7325), 807.

Ichikawa, H., Tsuchiya, T. & Tange, Y., 2014. The P-V-T equation of state and thermodynamic properties of liquid iron, *J. geophys. Res.,* **119**(1), 240–252.

Irving, J.C.E., Cottaar, S. & Lekić, V., 2018. Seismically determined elastic parameters for Earth's outer core, *Sci. Adv.,* **4**(6), eaar2538.

Kanamori, H. & Anderson, D.L., 1977. Importance of physical dispersion in surface wave and free oscillation problems, *Rev. Geophys.,* **15**(1), 105–112.

Kaneshima, S. & Helffrich, G., 2013. Vp structure of the outermost core derived from analysing large-scale array data of SmKS waves, *J. geophys. Int.,* **193**(3), 1537–1555.

Kaneshima, S. & Matsuzawa, T., 2015. Stratification of earth's outermost core inferred from SmKS array data, *Prog. Earth planet. Sci.,* **2**(1), 15.

Kaneshima, S., 2018. Array analyses of SmKS waves and the stratification of Earth's outermost core, *Phys. Earth planet. Inter.,* **276,** 234–246.

Kennett, B.L.N., Engdahl, E.R. & Buland, R., 1995. Constraints on seismic velocities in the Earth from traveltimes, *J. geophys. Int.,* **122**(1), 108–124.

Knittle, E. & Jeanloz, R., 1991. Earth's core–mantle boundary: results of experiments at high pressures and temperatures, *Science,* **251**(5000), 1438–1443.

Koelemeijer, P., Deuss, A. & Ritsema, J., 2013. Observations of core–mantle boundary Stoneley modes, *Geophys. Res. Lett.,* **40**(11), 2557–2561.

Kustowski, B., Ekström, G. & Dziewonski, A.M., 2008. Anisotropic shear-wave velocity structure of the Earth's mantle: a global model, *J. geophys. Res.,* **113**(B6), doi:10.1029/2007JB005169.

Lay, T. & Young, C. J., 1990. The stably–stratified outermost core revisited, *Geophys. Res. Lett.,* **17**(11), 2001–2004.

Lay, T., 2015. Deep Earth structure: lower mantle and D″, in *Treatise on Geophysics,* pp. 683–724, ed. Schubert, G., Elsevier.

Masters, G., Barmine, M. & Kientz, S., 2011. *Mineos,* California Institute of Technology.

Masters, T.G. & Widmer, R., 1995. Free oscillations: frequencies and attenuations, in *Global Earth Physics: A Handbook of Physical Constants*, AGU Reference Shelf 1, pp. 104–125, ed. Ahrens T. J., AGU.

Montagner, J.P. & Kennett, B.L.N., 1996. How to reconcile body-wave and normal-mode reference Earth models, *J. geophys. Int.,* **125**(1), 229–248.

Müller, G., 1985. The reflectivity method: a tutorial, *J. Geophys.,* **58,** 153–174.

Mound, J., Davies, C., Rost, S. & Aurnou, J., 2019. Regional stratification at the top of Earth's core due to core–mantle boundary heat flux variations, *Nat. Geosci.,* **12,** 575–580.

Olson, P., Landeau, M. & Reynolds, E., 2019. Outer core stratification from the high latitude structure of the geomagnetic field, *Front. Earth Sci.,* **6,** doi:10.3389/feart.2018.00140.

Resovsky, J.S. & Ritzwoller, M.H., 1998. New and refined constraints on three–dimensional Earth structure from normal modes below 3 mHz, *J. geophys. Res.,* **103**(B1), 783–810.

Ritsema, J., Deuss, A., Van Heijst, H.J. & Woodhouse, J.H., 2011. S40RTS: a degree–40 shear–velocity model for the mantle from new Rayleigh wave dispersion, teleseismic traveltime and normal–mode splitting function measurements, *J. geophys. Int.,* **184**(3), 1223–1236.

Rost, S. & Thomas, C., 2002. Array seismology: methods and applications, *Rev. Geophys.,* **40**(3), 2–1-2-27.

Schweitzer, J., Fyen, J., Mykkeltveit, S., Kværna, T. & Bormann, P., 2002. Seismic arrays, in *IASPEI New Manual of Seismological Observatory Practice,* pp. 1–51, IASPEI.

Souriau, A. & Poupinet, G., 1991. A study of the outermost liquid core using differential travel times of the SKS, SKKS and S3KS phases, *Phys. Earth planet. Inter.,* **68**(1–2), 183–199.

Tanaka, S. & Hamaguchi, H., 1993. Velocities and chemical stratification in the outermost core, *J. Geomag. Geoelectr.,* **45**(11–12), 1287–1301.

Tanaka, S., 2007. Possibility of a low P-wave velocity layer in the outermost core from global SmKS waveforms, *Earth planet. Sci. Lett.,* **259**(3–4), 486–499.

Tang, V., Zhao, L. & Hung, S.H., 2015. Seismological evidence for a non-monotonic velocity gradient in the topmost outer core, *Scient. Rep.,* **5,** 8613.

Vinet, P., Ferrante, J., Rose, J.H. & Smith, J.R., 1987. Compressibility of solids, *J. geophys. Res.,* **92**(B9), 9319–9325.

Wysession, M.E., Lay, T., Revenaugh, J., Williams, Q., Garnero, E.J., Jeanloz, R. & Kellogg, L.H., 1998. The D″ discontinuity and its implications, *Core-Mantle Bound. Region,* **28,** 273–297.

SUPPORTING INFORMATION

Supplementary data are available at *GJI* online.

Figure S1. SmKS differential traveltime measurements of Kaneshima & Matsuzawa (2015) with respect to PREM predictions. Predictions for outer-core models KHOMC and EPOC-Vinet are also shown, as well as predictions for PREM with a 280-km-thick D″-layer with ±3 per cent v_p and ±3 per cent v_s.

Figure S2. SmKS differential traveltime measurements of Kaneshima (2018) with respect to PREM predictions. Predictions for outer-core models KHOMC and EPOC-Vinet are also shown, as well as predictions for PREM with a 280-km-thick D″-layer with ±3 per cent v_p and ±3 per cent v_s.

Figure S3. Velocity in the top-500 km of the outer core according to several models: KHOMC, EPOC-Vinet, AK135 (Kennett *et al.* 1995) and PREM (Dziewonski & Anderson 1981). The solid green line shows the estimated model.

Figure S4. Predicted SmKS differential traveltimes as a function of epicentral distance for several outer-core velocity models, for (a) S3KS–S2KS, (b) S4KS–S3KS and (c) S5KS–S3KS with respect to differential times for PREM. The upper grey line denotes predictions for PREM with a 280-km-thick D″-layer with −3 per cent v_p and v_s; the lower grey line for a 280-km-thick D″-layer with +3 per cent v_p and v_s. Predictions for PREM with KHOMC in the outer core are in blue and predictions in red are for PREM with EPOC-Vinet in the outer core. The green dashed line shows the predictions for the estimated model and the data are from Kaneshima & Helffrich (2013).

Figure S5. Centre frequency shifts with respect to PREM frequencies for (a) outer-core sensitive modes and (b) Stoneley modes and first overtones. Predictions are shown for PREM with KHOMC, EPOC-Vinet's velocity model and the estimated model in the outer core. Data in (a) have been assembled by Irving *et al.* (2018) from various studies and the additional data in (b) are from Koelemeijer *et al.* (2013).

Figure S6. Predicted SmKS differential traveltimes as a function of epicentral distance for PREM with CMB depths of 2981 ± 0.5 and 2981 ± 5 km, for (a) S3KS–S2KS, (b) S4KS–S3KS and (c) S5KS–S3KS with respect to differential times for PREM. Measurements from Kaneshima & Helffrich (2013) are also shown.

Figure S7. Centre frequency shifts with respect to PREM frequencies for (a) Stoneley modes and a selection of first overtones and (b) outer-core sensitive modes. Predictions are shown for PREM with CMB depths of 2981 ± 5 and 2981 ± 0.5 km. The Stoneley-mode measurements in (a) are from Koelemeijer *et al.* (2013), the additional measurements in (a) as well as all measurements in (b) have been assembled by Irving *et al.* (2018) from various studies.

Please note: Oxford University Press is not responsible for the content or functionality of any supporting materials supplied by the authors. Any queries (other than missing material) should be directed to the corresponding author for the paper.